Talanta 117 (2013) 203–208

Contents lists available at ScienceDirect

Talanta

journal homepage: www.elsevier.com/locate/talanta

Au–Ag–Au double shell nanoparticles-based localized surface plasmon resonance and surface-enhanced Raman scattering biosensor for sensitive detection of 2-mercapto-1-methylimidazole

Xue Liao, Yanhua Chen, Meihong Qin, Yang Chen, Lei Yang, Hanqi Zhang, Yuan Tian *

College of Chemistry, Jilin University, Changchun 130012, PR China

ARTICLE INFO

Article history:
Received 20 May 2013
Received in revised form
21 August 2013
Accepted 28 August 2013
Available online 14 September 2013

Keywords:
Localized surface plasmon resonance (LSPR)
Surface-enhanced Raman scattering (SERS)
Au–Ag–Au double shell nanoparticles
2-Mercapto-1-methylimidazole (methimazole)

ABSTRACT

In this paper, Au–Ag–Au double shell nanoparticles were prepared based on the reduction of the metal salts $HAuCl_4$ and $AgNO_3$ at the surface of seed particles. Due to the synergistic effect between Au and Ag, the hybrid nanoparticles are particularly stable and show excellent performances on the detection of 2-mercapto-1-methylimidazole (methimazole). The binding of target molecule at the surface of Au–Ag–Au double shell nanoparticles was demonstrated based on both localized surface plasmon resonance (LSPR) and surface-enhanced Raman scattering (SERS) spectra. The LSPR intensity is directly proportional to the methimazole concentration in the range of $0.10–3.00 \times 10^{-7}$ mol L^{-1}. The SERS spectrum can be applied in identification of methimazole molecule. The LSPR coupled with SERS based on the Au–Ag–Au double shell nanoparticles would be very attractive for the quantitative determination and qualitative analysis of the analytes in medicines.

1. Introduction

In recent years, the rapid development of nanotechnology is related to the gold nanoparticles. Gold nanoparticles have small size, surface and quantum size effect. The metal nanoparticles have been used in chemical and biological detection [1,2]. Gold nanoparticles exhibit well-defined optical properties on account of their localized surface plasmon resonance (LSPR) and surface-enhanced Raman scattering (SERS) phenomena and develop rapidly [3,4]. LSPR arises from the resonant oscillation of conduction electrons on the surface of metal nanoparticles [5]. When the incident light frequency and the free electron collective oscillation frequency are the same, resonance can be produced. In aqueous solution, gold nanoparticles exhibit strong plasmon bands that are depended on their geometric shape, core–shell structure, size and the surrounding medium conditions [6–8]. LSPR of metal nanoparticles, especially gold and silver nanoparticles, is very sensitive to their surface-bound molecules and the surrounding environment. The LSPR spectrum of the noble metal nanoparticles is related to the dielectric constant of the surrounding environment. Because methimazole has C=N and C–N groups, LSPR effect highly related to the dielectric constant. Therefore, the adsorptions of chemical substances or biomolecules to surfaces of metal nano-structures can be detected by measuring the absorption or extinction spectra since the molecular adsorption gives rise to an increase in the dielectric constant near the surface. This shift can be described by measuring the change either in the peak intensity or in the peak location [9]. Although LSPR can be used to monitor the binding of macromolecules to functionalized nanoparticle surfaces, extinction spectroscopy does not allow for specific identification of the chemical entity. Vibrational spectroscopy, on the other hand, is capable of revealing molecular characteristics of the analyte. SERS is a surface sensitive technique that results from the enhancement of Raman scattering by molecules adsorbed on rough metal surface [10,11]. Individual bands in a SERS spectrum are characteristic of a specific molecular motion. The two well-known mechanisms to account for the origin of SERS are the electromagnetic and chemical or charge transfer mechanisms [12,13]. The enhancement factor can be as much as 10^{14}–10^{15}, which allows the technique to be sensitive enough to detect single molecule [11]. By combining SERS and LSPR spectroscopies, the detection and structural identification of molecules can be made.

Gold nanostructures were widely used for fabrication of sensor based on the LSPR optical characteristics. Gold nanostructures, especially, core–shell nanoparticles have been applied to many fields and received the critical attention because their optical properties depend on the shape and size of the nanostructures. The core–shell nanoparticles can be prepared by several methods [14–20]. However, the most common preparation method is wet chemical synthesis [21–23]. Depending on the synthesis procedure, successive reduction

* Corresponding author. Tel.: +86 431 85168399; fax: +86 431 85112355.
E-mail address: tianyuan@jlu.edu.cn (Y. Tian).

0039-9140/$ - see front matter © 2013 Elsevier B.V. All rights reserved.
http://dx.doi.org/10.1016/j.talanta.2013.08.051

gives the core–shell nano-particles which are attracting special attention owing to their unique plasmonic properties, fascinating optical, electronic, and catalytic properties [24], which are different from the individual metallic counterpart. These interesting physicochemical properties appear because of the combination of two kinds of metals and their fine structures, evolving new surface characteristics. Thus, core–shell nanoparticles, composed of two different metal elements, are of more interest compared with monometallic nanoparticles. Core–shell Au–Ag and core–shell Ag–Au are relatively conventional core–shell structures of the nanoparticles. The multicomponent systems can be used in variety of fields such as therapeutics, design of optoelectronic, magnetic and semiconductor materials.

Methimazole is an important thiol compound and has high efficiency in the treatment of hyperthyroidism in humans which has become the endocrine system disease of the 2nd big disease in the global scope nowadays [25]. To take too much methimazole can cause some symptoms of nausea, diarrhea, dizziness and even will appear vasculitis, lupus erythematous syndrome, nephritis and thrombocytopenia etc. Therefore it is necessary to quickly determine methimazole in tablets. Some methods have been reported for the determination of methimazole, including the electrochemical method [26], flow-injection spectrophotometry [27], HPLC–MS [28], the fluorescence probe method [29], chemiluminescence analysis [30] and LC [31]. However, there are still some limits in these methods. One important limit on HPLC and spectrometric techniques is that methimazole lacks sufficient UV absorption and thus to select a suitable mobile phase and a suitable reactant is required, which obviously results in increase in costs and analytical complexity. The LSPR of nanoparticles can be readily measured by UV–vis spectrometry and a delicate optical coupler is not required. Furthermore, fabrication of the sensors is very cheap and easy and can be finished in conventional chemical laboratories. In particular, it can provide good selectivity and sensitivity without the labeling process. Methimazole can be bound to the surface of gold nanoparticles strongly by Au–S which induces the change of LSPR intension.

In the present work, monodispersed Au seeds were synthesized, and then the metal salt $AgNO_3$ at the surface of Au seeds was reduced to form uniform Au–Ag core–shell. Subsequently, the Au–Ag core–shell was covered with second Au shell through the reduction of $HAuCl_4$ by ascorbic acid to form defect-free Au–Ag–Au double shell nanoparticles. The Au–Ag–Au double shell nanoparticles were used as probes to detect medicinal molecules. We studied the adsorption of methimazole on gold nanospheres and Au–Ag–Au double shell nanoparticles. The method for determining and identifying the methimazole was developed. The present method was applied to the analysis of the real samples. The experimental results indicated that the present method had some advantages in sensitivity, simplicity, rapidity and stability.

2. Material and methods

2.1. Materials

Tetrachloroauric acid ($HAuCl_4 \cdot 4H_2O$, 99.99%), trisodium citrate dihydrate, silver nitrate ($AgNO_3$, 99%), cetyltrimethylammonium bromide (CTAB, 99%), L-ascorbic acid (vitamin C) and 2-mercapto-1-methylimidazole were purchased from Beijing Ding Guo Biotech. Co. Ltd., China. $Al(NO_3)_3 \cdot 9H_2O$, $BaCl_2 \cdot 2H_2O$, $CaCl_2 \cdot 2H_2O$, $Cd(NO_3)_2 \cdot 4H_2O$, $CuCl_2 \cdot 2H_2O$, KCl, $MgCl_2 \cdot 6H_2O$, $NiCl_2 \cdot 6H_2O$, NaCl and $ZnSO_4 \cdot 7H_2O$ were purchased from Beijing Chemical Reagent Company (Beijing, China). The Britton–Robinson (BR) buffer solution (ionic strength, 0.5) contained 0.04 mol L^{-1} H_3PO_4, 0.04 mol L^{-1} HAc, and 0.04 mol L^{-1} H_3BO_3 and the pH values of the buffer solution were adjusted to appropriate pH using 0.2 mol L^{-1} NaOH. BR buffer solution was used to control the acidity of the interaction system. Aqua regia solution was used to clean the glassware. Other chemicals used here were of analytical reagent grade and all the solutions used in this study were prepared with ultrapure water.

2.2. Equipments

Absorption spectra were recorded on an Australian GBC Cintra 10e UV–vis–NIR spectrometer within the wavelength range from 400 to 1000 nm. The TEM image was obtained with a Hitachi H 800 transmission electron microscope operated at an accelerating voltage of 200 kV. The Raman spectra were recorded on a BTR111 MiniRam (B&W Tek, Inc.) equipped with 785 nm excitation laser and a 1 cm quartz cell. The laser power was chosen as 105 mW and the integration time was 10 s.

2.2.1. Preparation of gold nanospheres

Gold nanospheres were synthesized based on the reduction of $HAuCl_4$ with citrate following the procedure described by Yu and coworkers with slight modification [32] and stored in a brown bottle at 4 °C. All glassware used in the preparation was thoroughly cleaned with aqua regia, rinsed with triply distilled water, and oven-dried prior to use. In a 250 mL round-bottom flask equipped with a condenser, 50 mL of 0.02% $HAuCl_4$ was heated to the boil with vigorous stirring. Rapid addition of 50 mL of 0.07% sodium citrate in the boiling solution resulted in a color change from pale yellow to claret-red. The solution was kept in boiling for 10 min. Then the heating stopped, and the stirring continued for an additional 15 min. The solution was cooled down to room temperature, and filtered through 0.22 μm filter membrane. The size and morphology of nanoparticles were characterized by transmission electron microscopy (TEM). The result obtained by TEM showed that the size of the gold nanospheres had a narrow distribution and the mean diameter of the gold nanospheres was about 18 nm.

2.2.2. Preparation of Au–Ag–Au double shell nanoparticles

Au–Ag–Au double shell nanoparticles were prepared based on a reduction of the metal salts $HAuCl_4$ and $AgNO_3$ at the surface of seed particles by the ascorbic acid method according to literature [33] with slight modification. The gold seeds were prepared by heating a mixture of 20 mL 0.5 mmol L^{-1} $HAuCl_4$ and 20 mL 1.7 mmol L^{-1} sodium citrate solution to boiling for about 20 min in a capped glass bottle. The solution was heated till it is stable reddish-pink color. After the solution cooled, this seed solution was used for the synthesis of Au–Ag–Au double shell nanoparticles.

In a 200 mL beaker, 200 mL of 50 mmol L^{-1} CTAB, 5 mL of 0.1 mol L^{-1} ascorbic acid and 1.5 mL of 10 mmol L^{-1} of $AgNO_3$ were added sequentially. Then an aliquot of 1.5 mL gold seeds was added into this beaker. The beaker was shaken vigorously and 1 mol L^{-1} NaOH was added dropwise (in 4–5 steps). The color of the solution changed from pink to yellow after adding NaOH. In this way, the seeds were coated with the first silver shell to develop Au–Ag (core–shell) nanoparticles. In order to get these particles covered with the second shell of gold, 100 mL of the above solution, 1.5 mL of 0.1 mol L^{-1} ascorbic acid and 200 uL 0.1 mol L^{-1} $HAuCl_4$ were added into a cup. The cup then was vigorously shaken along with the color change from yellow to dark blue, which indicated the formation of the Au–Ag–Au double shell nanoparticles. The solution was then centrifuged at 20,000 rpm for 10 min twice to remove the excessive CTAB and the precipitation was re-dispersed in ultrapure water via the ultrasound.

2.3. Determination of methimazole

The stock solution of 2 mmol L^{-1} methimazole was prepared by dissolving methimazole in ultrapure water. The working solution of methimazole was prepared by diluting the stock solution with ultrapure water. The appropriate volume of Au–Ag–Au double shell nanoparticles or gold nanospheres suspension, 200 uL of BR buffer solution and appropriate volume of sample solution were added into a 5 mL test tube. The solution was mixed thoroughly with gentle shaking, and then diluted to 2 mL with double distilled water. The resulting solution was allowed to stand for the appropriate time at room temperature and the absorption spectrum of the solution was recorded with 1 cm path-length cell.

2.4. Preparation of sample solution

Two kinds of commercial tablets containing methimazole were accurately weighed, ground and transferred into a 50 mL flask, and then dissolved with double distilled water. The flask was ultrasonically shaken for about 15 min. The solution was diluted to 50 mL with ultrapure water. The resulting sample solution was diluted with ultrapure water and filtered before analysis.

2.5. Sample preparation for SERS analysis

700 μL colloidal solution of Au–Ag–Au double shell nanoparticles was incubated with a certain volume of sample solution in the 5 mL of centrifuge tube. 200 μL of buffer solution, 80 μL of 1 mol L^{-1} NaCl solution was added into the mixture. The solution was mixed thoroughly with gentle shaking, and then diluted to 2 mL with double distilled water. The resulting solution was allowed to stand for the appropriate time at room temperature and then detected with 1 cm quartz cell of Raman.

3. Results and discussion

3.1. UV–vis–NIR spectral characterization of gold nanoparticles

The uniform size and shape of the Au–Ag–Au double shell nanoparticles allow us to investigate the influence of shell and core on the LSPR. Fig. 1 shows the UV/vis spectra of colloidal Au, Ag, Au–Ag, and Au–Ag–Au double shell nanoparticles. The as-synthesized Au–Ag–Au double shell nanoparticles are in average size 73 nm. The absorption maxima of colloidal suspension of Ag nanoparticles is at around 400 nm. The Au core with the average size of 18 nm exhibits a LSPR peak at 520 nm. After coating with silver, a LSPR peak emerged at 450 nm was observed. The nanoparticles turned yellowish and greenish which also indicate formation of core–shell structure. When the second shell of gold can be formed on the first silver shell, the LSPR peak shows tremendous change. One new peak emerges at 602 nm with the color change from yellowish and greenish to dark blue.

It can be seen from Fig. 2 that Au–Ag–Au double shell nanoparticles and gold nanospheres in the absence of methimazole exhibit absorption peaks at 602 nm and 520 nm, respectively. The narrow peaks indicate that the naoparticles do not congregate in the solution. When methimazole was added into the solutions containing Au–Ag–Au double shell nanoparticles and gold nanospheres, the new peaks located at around 857 nm and 650 nm can be observed, respectively and the intensities of the peaks increase with the increase of methimazole concentration, which indicates the aggregation of the naoparticles.

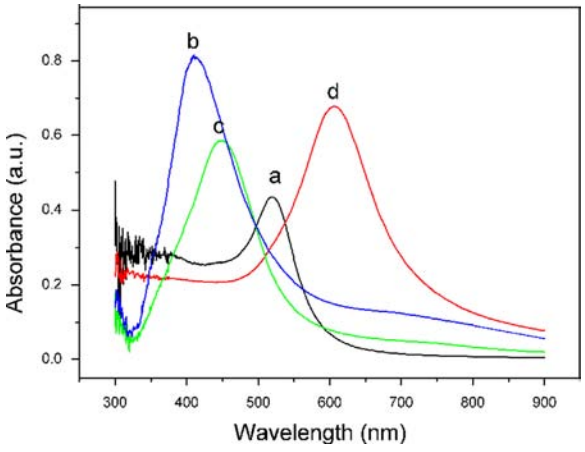

Fig. 1. UV/vis spectra of Au (a), Ag (b), Au–Ag (c) and Au–Ag–Au double shell (d) nanoparticles.

3.2. TEM observation of gold nanoparticles

The morphologies of the nanocomposites were characterized by TEM. Fig. 3 provides the TEM photographs of the prepared gold nanospheres and Au–Ag–Au double shell nanoparticles. The average particle sizes are about 18 nm and 73 nm, respectively. Fig. 3(a) and (c) shows TEM image of the double shell nanoparticles and gold nanospheres in the absence of methimazole, respectively. The TEM photographs show a relatively homogeneous distribution

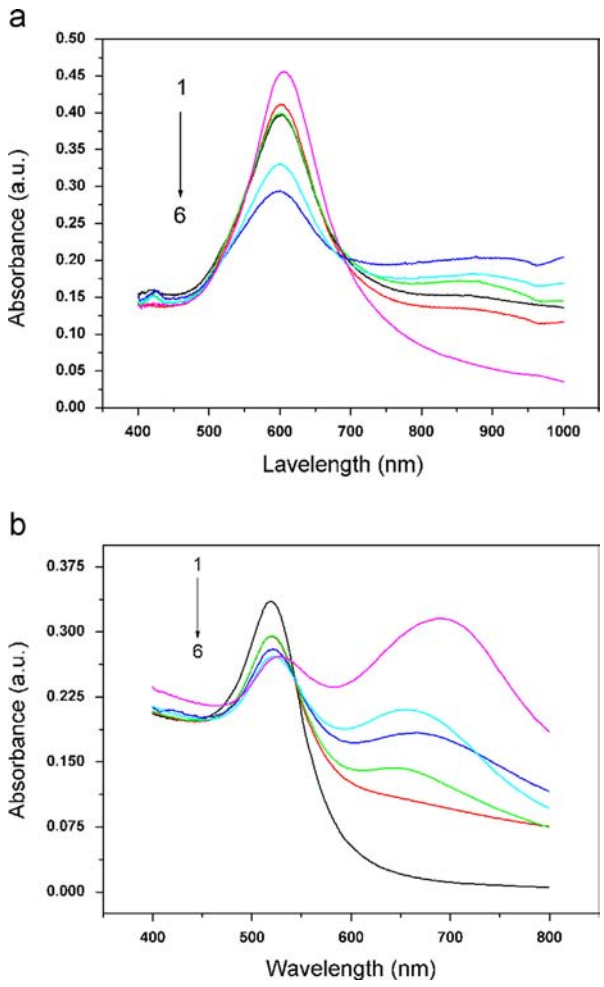

Fig. 2. Absorption spectra of Au–Ag–Au double shell nanoparticles (a) and gold nanosphere (b) in the presence of different methimazole concentrations. Concentrations of methimazole from (1 to 6) (a) 0.0, 0.1, 0.3, 0.5, 1.0 and 3.0×10^{-7} mol L^{-1} and (b) 0.0, 0.5, 1, 2, 3 and 5.0×10^{-7} mol L^{-1}.

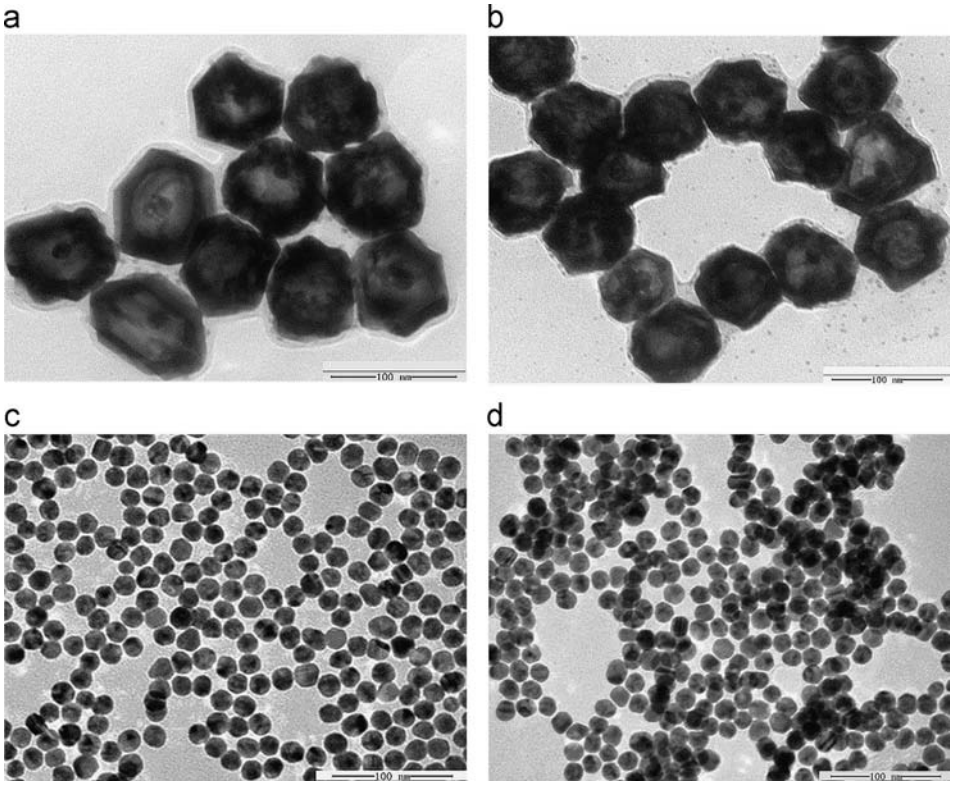

Fig. 3. TEM images of Au–Ag–Au double shell nanoparticles (a, b) and gold nanosphere (c, d) in the absence (a, c) and presence (b, d) of methimazole.

of particles. The Au–Ag–Au double shell nanoparticles have the advantages of Au and Ag nanoparticles. Due to the good stability and biocompatibility of Au shell and high sensitivity of Ag, the nanocomposites can be very stable and have high sensitivity and good biocompatibility. Compared with Au, the Ag shows a higher enhancement in the visible light region. However, it should be noted that Ag is unstable and not biocompatible. Therefore, Au was used as the protective agent for the Ag nanoparticles and the underneath Ag may provide extra enhancement of sensitivity of the biosensor. It also can be shown from Fig. 3(b) and (d) that after addition of methimazole, the Au–Ag–Au double shell nanoparticles and gold nanospheres occur aggregated in the solutions. The reason mainly is that in the presence of methimazole, the surface of Au–Ag–Au double shell nanoparticles adsorbs methimazole by Au–S covalent bond.

3.3. Optimization of experimental conditions

3.3.1. Effect of pH

BR buffer solution was used to adjust the pH value of the analytical solution. Fig. 4 shows the effect of the pH value on the LSPR intensity of the system. The absorbance ratio A_{870}/A_{602} for the Au–Ag–Au double shell nanoparticles in the presence of methimazole increases with the increase of pH value, reaches the maximum at pH 4.5, and then decreases slightly. Because Au–Ag–Au double shell nanoparticles are positively charged due to the adsorption of the positively charged surfactant CTAB on the surface of the nanoparticles and high pH value can induce the aggregation of Au–Ag–Au double shell nanoparticles, the absorption spectra change. So pH 4.5 of BR buffer solution was selected for the determination of methimazole.

The gold nanospheres are negatively charged due to the adsorption of citrate groups, which is responsible for the stability of colloidal gold. It can be seen from Fig. 4 that the A_{650}/A_{520} of gold nanospheres in the presence of methimazole increases with

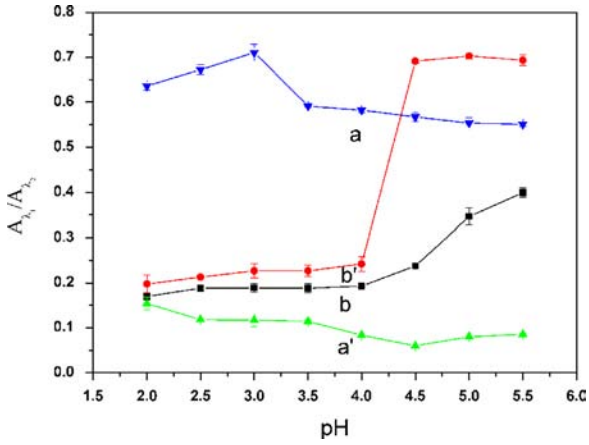

Fig. 4. Influence of pH value on the $A_{\lambda 1}/A_{\lambda 2}$ of nanoparticles (a, b) and nanoparticle-methimazole (a′, b′) system. The $A_{\lambda 1}/A_{\lambda 2}$ represents A_{650}/A_{520} for gold nanosphere (a and a′), and the A_{870}/A_{602} for Au–Ag–Au double shell nanoparticles (b and b′).

the increase of pH value and reaches a maximum at the pH value of 3.0. At the same time, when the pH value is lower than 3.0, the color of solution changes obviously and when the value of pH is higher than 3.0, there is a systematic red shift of the absorption peak and A_{650}/A_{520} decreases slightly. The gold nanospheres in the presence of methimazole can be aggregated and have a strong absorption signal of LSPR at pH value of 3.0. So pH 3.0 was selected when gold nanospheres were used.

3.3.2. Incubation time

The effect of the incubation time on the LSPR intensity of nanoparticles in the absence and presence of methimazole was investigated. Fig. 5 shows that absorbance ratios of the Au–Ag–Au double shell nanoparticles and gold nanospheres change slightly

with increase of incubation time. However, the A_{870}/A_{602} of Au–Ag–Au double shell nanoparticles in the presence of methimazole reaches a clear-cut plateau in 15 min at room temperature and remains unchanged after 15 min. Therefore, 15 min was selected in this method. As shown in Fig. 5, the reaction between gold nanospheres and methimazole is rapid and gold nanospheres can achieve the best coagulation in a short period of time. The A_{650}/A_{520} of the system reaches a maximum at 5 min and after 5 min the absorbance ratio decreases slightly. So, the incubation time 5 min was selected in this assay.

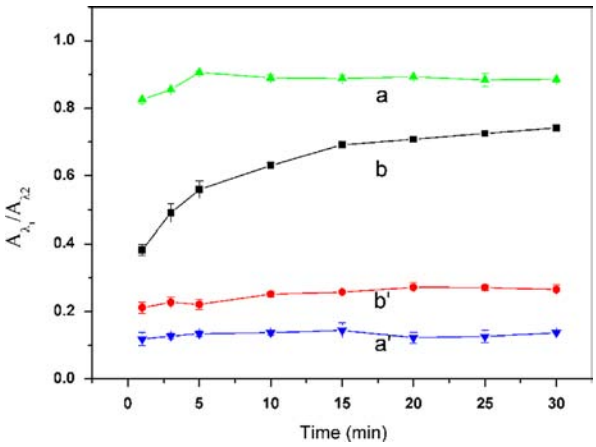

Fig. 5. Effect of incubation time on the $A_{\lambda 1}/A_{\lambda 2}$ of nanoparticles (a and b) and nanoparticle-methimazole (a′ and b′) system. The $A_{\lambda 1}/A_{\lambda 2}$ represents the A_{650}/A_{520} for gold nanosphere (a and a′) and A_{870}/A_{602} for Au–Ag–Au double shell nanoparticles (b and b′).

Table 1
Influence of coexisting substances.

Substance	Concentration (10^{-6} mol L)	Shift of $A_{\lambda 1}/A_{\lambda 2}$(%)	
		Gold nanosphere	Au–Ag–Au double shell nanoparticles
K^+, Cl^-	15	5.5	2.9
Ba^{2+}, Cl^-	30	−2.4	0.3
Ca^{2+}, Cl^-	25	−2.3	−0.9
Cu^{2+}, Cl^-	25	6.1	4.5
Mg^{2+}, Cl^-	25	−2.6	−2.6
Na^+, Cl^-	15	−6.7	0.8
NH_4^+, Cl^-	10	3.4	−3.1
Pb^{2+}, NO_3^-	5	4.5	−4.1
Al^{3+}, NO_3^-	10	4.5	−4.2
Cr^{3+}, NO_3^-	3	6.1	−0.7
Glucose	8	7.0	3.5
L-Lysine	8	6.2	1.3
L-Serine	10	2.6	1.8
L-Proline	10	6.3	3.5
L-Cysteine	0.5	4.4	−1.1
Albumin	0.07 ug mL	4.8	0.7

3.4. Effect of coexisting substances

The coexisting substances with positive or negative charges will have an effect on the LSPR intensity. When the concentration of methimazole was 3×10^{-7} mol L^{-1}, the effects of the foreign substances including metal ions and protein were tested. The experimental results are shown in Table1. It can be seen that most of the foreign substances have little influence on the LSPR intensity of this system and can be allowed at high concentration levels. At the same time, selectivity of the Au–Ag–Au double shell nanoparticles is higher selectivity than that of gold nanospheres.

3.5. The calibration curves

Under the optimum conditions, the calibration curves for determination of methimazole were constructed. The regression equations are shown in Table 2. When the Au–Ag–Au double shell nanoparticles are used, the absorbance ratios are directly proportional to the methimazole concentrations in the range of 0.10–3.00 × 10^{-7} mol L^{-1}. The correlation coefficient is 0.998 and there is a good linear relationship between the absorbance ratio of A_{870}/A_{602} and methimazole concentration. When the gold nanospheres were used, there is a linear relationship between the absorbance ratio of A_{650}/A_{520} and the concentration of methimazole in the range of 0.50–5.00 × 10^{-7} mol L^{-1}. The corresponding correlation coefficient is 0.997, which indicates that there is a good linear relationship between the absorbance ratios and methimazole concentration. It can be concluded that compared with gold nanospheres, when Au–Ag–Au double shell nanoparticles were used, the sensitivity for the determination of methimazole was higher and the linear range was wider.

3.6. Analytical application

To evaluate the analytical applicability of the present method, the method was applied for the determination of methimazole in commercial tablets. The results are shown in Table 3. When the Au–Ag–Au double shell nanoparticles were used, the recoveries of the analyte in the two samples are 97.0% and 98.9%, and the RSDs are 2.82 and 2.35, respectively. When the gold nanospheres were used, the recoveries are 95.2% and 97.6%, and the RSDs are 3.39 and 2.83 respectively. The recoveries obtained with the Au–Ag–Au double shell nanoparticles are slightly higher than those obtained with the gold nanospheres.

3.7. SERS bands of methimazole

LSPR can be used for detecting surface binding or release of molecules. However, this method is unable to identify the chemical entity of the molecule that binds to the surface. SERS, on the other hand, is capable of revealing molecular characteristics of the analyte. In our preliminary studies, Au–Ag–Au double shell nanoparticles were used as the substrate because Au–Ag–Au double shell nanoparticles have a broad range of excitation wavelengths can be used for a SERS experiment. Methimazole can bond to the second shell of gold surface through charge-transfer (covalent bond).

Table 2
The calibration curves of methimazole.

Gold nanoparticles	Linear range (10^{-7}mol L^{-1})	Regression equation [a]	Correlation coefficients (r)	Detection limits (10^{-7}mol L^{-1})
Au–Ag–Au double shell nanoparticles	0.10–3.00	$y=0.136x+0.294$	0.998	0.024
Gold nanospheres	0.50–5.00	$y=0.189x+0.133$	0.997	0.074

[a] x stands for the test concentration; y stands for absorbance ratio.

Table 3
Analytical results of methimazole in real samples.

Sample	Gold nanoparticles	Added (10^{-7}mol L)	Found (10^{-7}mol L)	Recovery ($n=3$, %)	RSD ($n=3$, %)	Relative error (%)
Table 1	Au–Ag–Au double shell nanoparticles	3.00	2.96	98.7	2.35	1.3
	Gold nanosphere	2.00	1.95	97.5	2.83	2.5
Table 2	Au–Ag–Au double shell nanoparticles	3.00	2.91	97.0	2.82	3.0
	Gold nanosphere	2.00	1.91	95.5	3.39	4.5

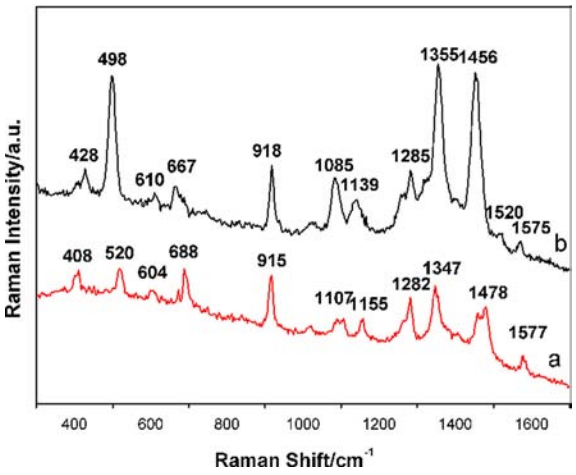

Fig. 6. Raman spectra of methimazole in aqueous solution (a) and SERS spectrum of methimazole in the presence of Au–Ag–Au double shell nanoparticles (b).

On the basis of previous reports [34,35], Fig. 6 shows the Raman spectra of methimazole in aqueous solution and SERS spectra of methimazole adsorbed onto Au–Ag–Au double shell nanoparticles. The difference of the spectra indicates that there is a very strong interaction between methimazole and Au–Ag–Au double shell nano-particles. There are many peaks in the SERS spectra of methimazole. The major peaks in these spectra are located at 428, 498, 610, 667, 918, 1085, 1139, 1285, 1355, 1456, 1520, and 1575 cm^{-1}. All these peaks are characteristic of chemisorbed methimazole molecules. A strong peak at 498 cm^{-1} is attributed to N–C–S bending. Of these peaks, the peak observed at 1456 correspond to C–S stretch, while the band at 1575 cm^{-1} corresponds to ring C–C stretch. The peaks at 1355 and 1285 cm^{-1} are contributed to the ring CN stretch with contributions from ring bending and ring CH bending vibrations. The medium peaks at 428, 610, 918, 1085, 1139, 1285, and 1456 cm^{-1} are attributed to the ring bending and breathing and ring CN stretching vibrations. These preliminary SERS data reflect the presence of methimazole on the Au–Ag–Au double shell nanoparticles. Because the present method is a couple of two methods, the analyte is determined quantitatively by LSPR and then qualitatively identified by SERS.

4. Conclusions

In this work, Au and Au–Ag–Au double shell nanoparticles were synthesized by successive reduction of the metal salts. Methimazole can be quantitatively determined by LSPR and qualitatively identified by SERS using Au–Ag–Au double shell nanoparticles and gold nanospheres as probe. Under the optimized conditions, the absorbance ratio of Au–Ag–Au double shell nanoparticles increases almost linearly with the increase of the concentration of methimazole in the range of 0.10–3.00 $\times$ 10^{-7} mol L^{-1}. The sensitivity obtained with Au–Ag–Au double shell nanoparticles is higher than that obtained with the gold nanospheres. Some real samples were analyzed and the results were satisfactory. The present method has the advantages of high sensitivity and low cost.

References

[1] E. Petryayeva, U.J. Krull, Anal. Chim. Acta 706 (2011) 8–24.
[2] K.A. Willets, R.P. Van Duyne, Annu. Rev. Phys. Chem. 58 (2007) 267–297.
[3] L. Rodriguez-Lorenzo, L. Fabris, R.A. Alvarez-Puebla, Anal. Chim. Acta 745 (2012) 10–23.
[4] I.M. White, S.H. Yazdi, W.W. Yu, Microfluid. Nanofluid. 13 (2012) 205–216.
[5] B. Sepúlveda, P.C. Angelomé, L.M. Lechuga, L.M. Liz-Marzán, Nano Today 4 (2009) 244–251.
[6] K.L. Kelly, E. Coronado, L.L Zhao, G.C. Schatz, J. Phys. Chem. B 107 (2003) 668–677.
[7] K.-J. Chen, C.-J. Lu, Talanta 81 (2010) 1670–1675.
[8] J.J. Mock, M. Barbic, D.R. Smith, D.A. Schultz, S. Schultz, J. Chem. Phys. 116 (2002) 6755–6759.
[9] G.J. Nusz, A.C. Curry, S.M. Marinakos, A Wax, A. Chilkoti, ACS Nano 3 (2009) 795–806.
[10] K. Kneipp, Y. Wang, H. Kneipp, L.T. Perelman, I. Itzkan, R.R. Dasari, M.S. Feld, Phys. Rev. Lett. 78 (1997) 1667–1670.
[11] S. Nie, S.R. Emory, Science 275 (1997) 1102–1106.
[12] M. Moskovits, Rev. Mod. Phys. 57 (1985) 783–826.
[13] A. Otto, I. Mrozek, H. Grabhorn, W. Akemann, Phys. Condens. Mater 4 (1992) 1143–1212.
[14] F. Douglas, R. Yañez, J. Ros, S. Marín, A.D.L. Escosura-Muñiz, S. Alegret, J. Nanopart. Res. 10 (2008) 97–106.
[15] K. Mallik, M. Mandal, N. Pradhan, T. Pal, Nano Lett. 1 (2001) 319–322.
[16] M. Treguer, C. de Cointet, H. Remita, J. Khatouri, M. Mostafavi, J. Amblard, J. Belloni, J. Phys. Chem. B 102 (1998) 4310–4321.
[17] K.I. Okazaki, T. Kiyama, K. Hirahara, N. Tanaka, S. Kuwabata, T. Torimoto, Chem. Commun. 6 (2008) 691–693.
[18] D. Ferrer, A. Torres-Castro, X. Gao, S. Sepúlveda-Guzmán, U. Ortiz-Mendéz, M. José-Yacamán, Nano Lett. 7 (2007) 1701–1705.
[19] M. Tsuji, N. Miyamae, K. Matsumoto, S. Hikino, T. Tsuji, Chem. Lett. 34 (2005) 1518–1519.
[20] F.-K. Liu, P.-W. Huang, Y.-C. Chang, F.-H. Ko, T.-C. Chu, Langmuir 21 (2005) 2519–2525.
[21] S. Link, Z.L. Wang, M.A. El-Sayed, J. Phys. Chem. B 103 (1999) 3529–3533.
[22] B. Rodriguez-Gonzalez, A. Burrows, M. Watanabe, C.J. Kiely, L.M. Liz-Marzán, J. Mater. Chem. 15 (2005) 1755–1759.
[23] M.Z. Liu, P. Guyot-Sionnest, J. Phys. Chem. B 108 (2004) 5882–5888.
[24] S. Pande, S.K. Ghosh, S. Praharaj, S. Panigrahi, S. Basu, S. Jana, A. Pal, T. Tsukuda, T. Pal, J. Phys. Chem. C 111 (2007) 10806.
[25] M. Garnera, D.R. Armstronga, J. Reglinskia, W.E. Smitha, R. Wilsonb, J.H. McKillopb, M. Bioorg, Chem. Lett. 4 (1994) 1357–1360.
[26] J.Y. Sun, C.Y. Zheng, X.L. Xiao, L. Niu, T.Y. You, E.K. Wang, Electroanalysis 17 (2005) 1675–1680.
[27] A. Economou, P.D. Tzanavaras, M. Notou, D.G. Themelis, Anal. Chim. Acta 505 (2004) 129–133.
[28] K. De Wasch, H.F. Be Brabander, S. Impens, M. Vandewiele, D. Courtheyn, J. Chromatogr. A 912 (2001) 311–317.
[29] F. Dong, K.W. Hu, H.Y. Han, J.G. Liang, Microchim. Acta 165 (2009) 195–201.
[30] Z.H. Sheng, H.Y. Han, G.D. Yang, Luminescence 26 (2011) 196–201.
[31] K. Kuśmierek, E. Bald, Talanta 71 (2007) 2121–2125.
[32] Z.-S. Wu, S.-B. Zhang, M.-M. Guo, C.-R. Chen, G.-L. Shen, R.-Q. Yu, Anal. Chim. Acta 584 (2007) 122–128.
[33] A. Knauer, A. Thete, S. Li, H. Romanus, A. Csáki, W. Fritzsche, J.M. Köhler, J. Chem. Eng. 166 (2011) 1164–1169.
[34] N. Biswas, S. Thomas, A. Sarkar, T. Mukherjee, S. Kapoor, J. Phys. Chem. C 113 (2009) 7091–7100.
[35] R. Zhang, Y. Wen, N. Wang, Y. Wang, Y.Y. Wang, Z.R. Zhang, H.F. Yang, J. Phys. Chem. B 114 (2010) 2450–2456.